

Effect of Clay Concentration on the Wear Behavior and Permeability of Polypropylene/Clay Nanocomposites

María Fernanda Horst,¹ Walter Tuckart,² Liliana Del Blanco,¹
Marcelo D. Failla,^{1,2} Lidia M. Quinzani¹

¹Planta Piloto de Ingeniería Química (PLAPIQUI), UNS-CONICET - C.C. 717 - Bahía Blanca 8000, Argentina

²Departamento de Ingeniería, Universidad Nacional del Sur (UNS), Alem 1253 - Bahía Blanca 8000, Argentina

Received 29 April 2011; accepted 29 September 2011

DOI 10.1002/app.36414

Published online 31 January 2012 in Wiley Online Library (wileyonlinelibrary.com).

ABSTRACT: The permeability and wear behavior of nanocomposites based on polypropylene (PP), polypropylene grafted with maleic anhydride (PPg), and montmorillonite (MMT) have been studied. Clay concentrations of 2–15 wt % and a constant PPg:MMT ratio of 3 : 1 were considered. The wear behavior of all materials was studied using the “pin-on-disc” technique. The results indicate that, for given clay concentration, the wear resistance decreases with applied load and that the composites are ~ 20 times more resistant than their matrices. Moreover, the wear rate of the nanocomposites decreases as the clay

concentration increases while that of the corresponding matrices increases. The PP, matrices, and composites display similar values of friction coefficient that neither changes with normal load. Additionally, the oxygen permeability of PP is gradually reduced by the increase of both clay and PPg concentration, being the effect of the filler tactoids much larger than that of the compatibilizer. © 2012 Wiley Periodicals, Inc. *J Appl Polym Sci* 125: E495–E502, 2012

Key words: nanocomposites; poly(propylene); montmorillonite; wear; barrier properties

INTRODUCTION

Polymer nanocomposites (PNCs) consist in low concentrations of inorganic particles of nanometer dimensions that are dispersed in polymeric matrices.^{1,2} Clays are the most commonly used inorganic fillers because of their laminated structure. PNCs have received much attention in recent years mainly because they have a large potential to reach properties similar to those of traditional compounds when using much smaller amounts of fillers.^{1,3–5} Particularly, the mechanical and barrier properties are specially mentioned in the literature as being capable to be improved. Additionally, the presence of nanoparticles also affects the morphology and the optical and rheological properties of the polymer matrix.

PNCs based in polypropylene (PP) and organomodified montmorillonite (o-MMT) are of particular interest mainly because both, the polymer and the filler, are extensively used inexpensive materials. Furthermore, PP has relatively good performance, in

terms of strength and processability, and the PP-based composites are being used in industry because of its high chemical and wear resistance.⁶ Previous works from the literature have demonstrated that the morphological, thermal, mechanical, and rheological properties of PP/MMT composites depend mainly on molecular weight and grafting degree of the added compatibilizer [grafted polypropylene (PPg)], concentration and type of intercalant used in the modification of the clay, relative concentrations PP/MMT and PPg/MMT, mixing conditions, and molecular weight of the PP.^{7–11}

In particular, the presence of the filler may affect the wear resistance of the polymer matrix. In general, the wear resistance of polymers in polymer-metal sliding contact is known to be related to friction-transfer and the formation of a polymer transfer film on the metal counterface.^{12–20} This film is controlled by the nature and roughness of the counterbody, as well as by the sliding conditions, such as velocity, contact stress level, atmosphere, and temperature, and the nature of the polymer. In most cases, the addition of a small amount of nanoparticles enhances the adhesion of the polymer to the counterface reducing the wear rate of the polymer. Furthermore, there are cases in which the filler decompose generating reaction products that enhance the bonding between the transfer film and the counterface, contributing to the reduction of the wear. In the case of clay-reinforced polymers, which

Correspondence to: L. M. Quinzani (lquinzani@plapiqui.edu.ar).

Contract grant sponsors: National Research Council of Argentina (CONICET), Universidad Nacional del Sur (UNS), Agencia Nacional de Promoción Científica y Tecnológica (ANPCyT).

have been widely used for different structural and technological applications, very few studies can be found that analyze the wear behavior of these materials¹⁷ and even less that deal with PNCs based on PP and MMT. Chen et al.²¹ analyzed the effect of o-MMT concentration on the friction and wear behavior of PP composites sliding against steel. According to the authors, composites containing 1.5 wt % of o-MMT exhibit higher tensile strength, hardness and much better friction, and wear behavior than the PP matrix. Moreover, they claim that, as the content of o-MMT increases, the wear mechanism gradually changes from adhesive to abrasive wear (at 4 wt % o-MMT). Similarly, Kanny et al.⁶ studied the wear behavior and mechanical properties of PP mixed with a commercial o-MMT using the pin-on-disk technique. They observe that the wear resistance of composites sliding against brass discs increases as the concentration of clay increases. Still, it should be mentioned that no exfoliation is observed by the authors above 1 wt % and a large proportion of small voids is seen at all clay concentrations. Kui et al.²² studied the wear behavior of PP composites based in two organomodified MMTs that were prepared through melt mixing in a twin-screw extruder. They observe that the friction coefficient and wear rate of both type of materials are lower than those of PP under water lubrication.

As already mentioned, other properties that may be improved by the presence of nanofillers are the barrier properties. Nanocomposites are multiphase materials in which the coexistence of phases with different sorption and diffusion properties can cause complex transport phenomena.³ The presence of silicate layers are expected to cause a decrease in permeability caused by the retarded diffusion of the molecules, which should follow more tortuous paths to bypass the filler. This phenomenon is enhanced when the filler is of nanometer size with high-aspect ratio.^{23–34} Most of the works in the literature that study PNCs based on PP and clay fillers agree in the fact that the permeability of the composites is lower than that of the polymeric matrix and it decreases up to ~ 30–50% as the clay concentration increases.^{27–34} These works performed permeation measurements based on small gases, like oxygen, nitrogen, carbon dioxide, water vapor, and helium, through compression molded membranes with up to 5–10 wt % clay concentration.

In the present article, we study melt-mixed blends of PP, PPg, and a commercial-modified MMT analyzing the effect of clay concentration on the tribological and barrier properties of these materials. The PPg is a maleic anhydride-grafted PP which is used to improve the dispersion of the organomodified clay in the low-polarity polymer. The wear resistance and the friction coefficient were determined using the pin-on-disk technique, measuring the final

weight loss and the friction force under different normal loads. On the other hand, the permeability of the blends against oxygen gas was investigated on compress-molded films. The structural characteristics and rheological properties of the PP/PPg/o-MMT nanocomposites considered in the present work were already presented in previous articles.^{8,9}

EXPERIMENTAL

Materials

The polymers used are an isotactic PP from Petroquímica Cuyo S.A.I.C. ($M_w = 330,000$ g/mol and $M_w/M_n = 4.7$) and a PPg from Uniroyal Chemical Co. (Polybond 3200, $M_w = 120,000$ g/mol, $M_w/M_n = 2.6$, 1 wt % of maleic anhydride). The clay used as reinforcement is a MMT modified with dimethyl dihydrogenated tallow ammonium chloride (Nanomer® I.44P from Nanacor). This clay has particle size in the range 15–25 μm , a modifier concentration of 1.04 meq/g of inorganic clay with surface coverage of about 70%, a decomposition temperature of 200°C, and 2.6 nm of interlayer spacing, d_{001} .^{8,9}

The PNCs were obtained by melt mixing the polymers with the clay in a Brabender Platograph mixer at 185°C during 15 min at 50 rpm under nitrogen atmosphere. The clay concentration was varied between 2 and 15 wt %, which corresponds to a concentration range of inorganic material of 1.3–9.5 wt %. The amount of PPg used in the blends determines a constant 3 : 1 ratio of PPg:o-MMT. Blends of PP and PPg with the proportions in which they appear in the PNCs were also prepared and tested.

According to previous results,^{8,9} the o-MMT used in the present study increases its interlayer spacing (from 2.6 to 3.3 nm) and displays partial intercalation and exfoliation after mixing with the polymers. The linear viscoelastic characterization shows evidence of percolation of clay tactoids at clay concentrations of ~ 10 and ~ 7 wt % in fresh samples obtained after mixing and in melt-annealed samples, respectively. The specimens used in the present study have not been annealed.

The composites are identified in the article as PC#, where # is a number that represents the concentration of clay. For example, PC2 is the material based in 2 wt % of MMT, 6 wt % of PPg, and 92 wt % of PP. mPC# is the nomenclature used to identify the mixtures of PP and PPg that correspond to the matrices of the PC# composites. For example, mPC2 is the mixture of PPg and PP in the same ratio that they appear in PC2.

Characterization

The wear and friction tests were performed on a “pin-on-disc” system that was built in our laboratories

in accordance with ASTM G99 standard. Each test consists in the unlubricated sliding of the flat face of a cylindrical polymeric pin over the surface of a metal disc. The 6-mm diameter and 15-mm length pins were prepared by injection molding using an ATLAS LMN system. Two steel discs (SAE 4140) of 40-mm diameter were used as counterbody: disk "A" ($R_a = 2.3 \mu\text{m}$ and $R_z = 12 \mu\text{m}$) and disk "B" ($R_a = 2.9 \mu\text{m}$ and $R_z = 15 \mu\text{m}$). The tests were performed at $23 \pm 2^\circ\text{C}$ using a constant rotating speed of 375 rpm during 40 min. The sliding distance was 1884 m in all cases. Normal loads of 2.5, 5, 7.5, 10, and 12.5 N were applied to the cylindrical pins. At least two specimens of each material were tested at each condition. The evolution of the friction force during each test was used to calculate the friction coefficient, while the final weight lost by each pin was used to determine the wear resistance. The wear results are presented in term of volume, which was calculated by converting the weight lost data with the density of the materials. The friction force was measured with a load cell attached to the sample support. The final state of the contact surface of the pins was observed by scanning electron microscopy (SEM) using a LEO EVO-40 XVP system operating at 15 kV. The steel counterface was also observed using an optical microscope.

The device used to measure the oxygen transmission rate through the polymeric films was a MOCON Ox-Tran 2/21. The permeability coefficient was calculated according the ASTM standard D3985, using an exposed film area of 5 cm^2 . The tests were performed at 23°C and 0% of RH using oxygen flow at 1 atm. The films, which were prepared by compression molding at 180°C , had thickness in the range 140–200 μm . The thickness variation among the specimens of a given material was no larger than 10 μm . These values were measured using a micrometer Mahr Millimar C 1208 and an Inductive Probe with an accuracy of 99.7%. Each permeability data presented in the article corresponds to the average of at least four measurements.

The heat of fusion and melting temperature of all materials were also measured. They were determined by differential scanning calorimetry (DSC) using a Perkin-Elmer Pyris I system with a heating rate of $10^\circ\text{C}/\text{min}$.

RESULTS AND DISCUSSION

Wear resistance

Figure 1 displays the volume loss of all analyzed materials as a function of applied load. For more clarity, the wear results of the PNCs are presented in Figure 1(b) while those of the corresponding matrices are in Figure 1(a). The data of PP are included

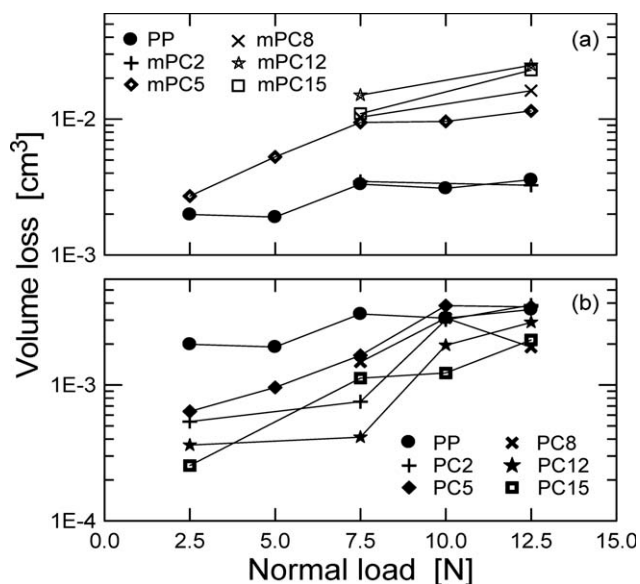


Figure 1 Volume loss as a function of applied normal load of PP and PP/PPg blends (a) and composites (b).

in both figures for comparison. PP, mPC5, and PC5 were tested at all loads using disc A, while the rest of the PNCs and matrices were examined using disc B. These last composites were tested with most normal loads while their matrices were tested using 7.5 and 12.5 N. To analyze the effect of the disc roughness, specimens of a few materials were also tested with both discs. Within experimental error, no significant difference was obtained among these measurements.

The data in Figure 1 show that, in general, the wear resistance of the materials decreases as the normal load increases. The data also reveal that, for a given normal load, the volume loss of the matrices is larger than that of the PP [Fig. 1(a)] while the addition of clay to the PP/PPg blends decreases the volume loss to values even lower than those of PP [Fig. 1(b)]. Furthermore, as the concentration of PPg increases in the PP/PPg blends, the wear increases (at least in the 7.5–12.5 N range considered). The opposite occurs as the concentration of clay increases. The effect of the presence of PPg may be justified by the difference in the average molecular weight of the polymers, and consequent melt viscosity that decreases as the concentration of PPg increases.^{8,35} Within the experimental error, the data of Figure 1 show that, as the clay concentration augments, the volume loss decreases and separates farther away from the data of the corresponding matrices. For example, at 7.5 N, the volume loss increases approximately five times when the PPg/PP ratio in the blends change from 6/92 (mPC2) to 45/40 (mPC15) and decreases approximately five times when the composite composition (MMT/PPg/PP) changes from 2/6/92 to 15/45/40.

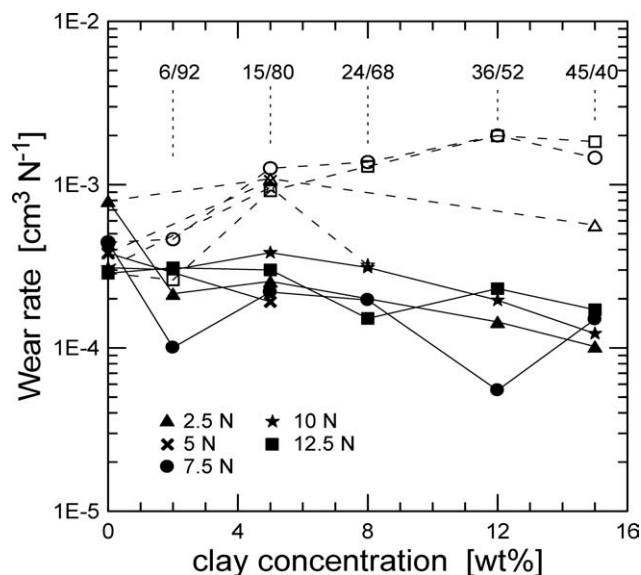


Figure 2 Wear rate as a function of clay concentration. Data of PNCs (full symbols) and their matrices (empty symbols) obtained using different normal loads. The corresponding PPg/PP ratios are displayed at the top of the figure.

The previous comments are better demonstrated in Figure 2, where the data of Figure 1 are presented as wear rate (i.e., volume loss/normal load) as a function of clay concentration. To facilitate the comparison, the data of the matrices are included in the figure, at the clay concentration of the corresponding PNC. This plot shows more clearly that the composites have lower wear rate than their matrices, and that, within experimental error, the difference between the values of the wear resistance of each PNC and its matrix becomes larger as the clay concentration increases.

During the sliding tests, the friction force is continuously registered as a function of time. These sig-

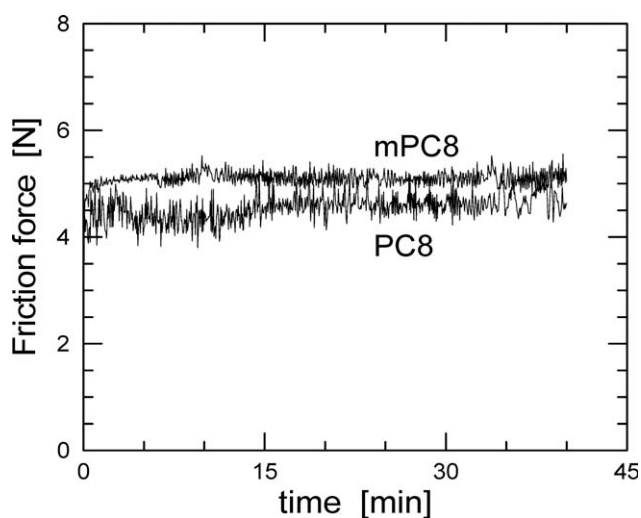


Figure 3 Friction force as a function of time. Data corresponding to PC8 and mPC8 under 12.5 N of normal force.

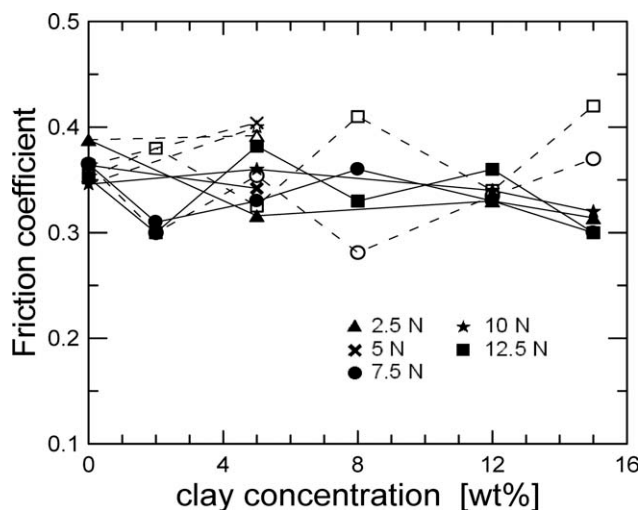


Figure 4 Friction coefficient as a function of clay concentration. Data of PNCs (full symbols) and their matrices (empty symbols) obtained using different normal loads.

nals normally present fluctuations around a practically constant mean value. The friction coefficient (friction force/normal load) of each material is then estimated from that mean value after steady state is

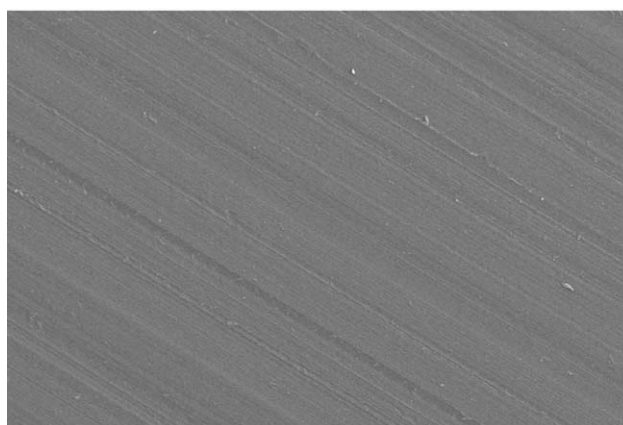
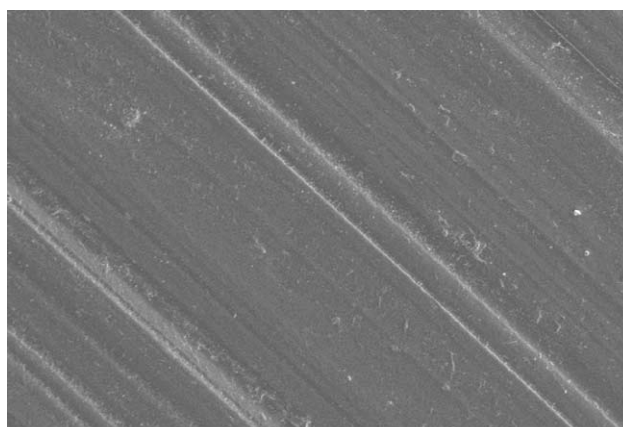


Figure 5 SEM micrographs of PC5 (left) and mPC5 (right) tested using 5 N of normal force. Size of the displayed zones: $307 \times 220 \mu\text{m}^2$ (magnification: $\times 1000$).

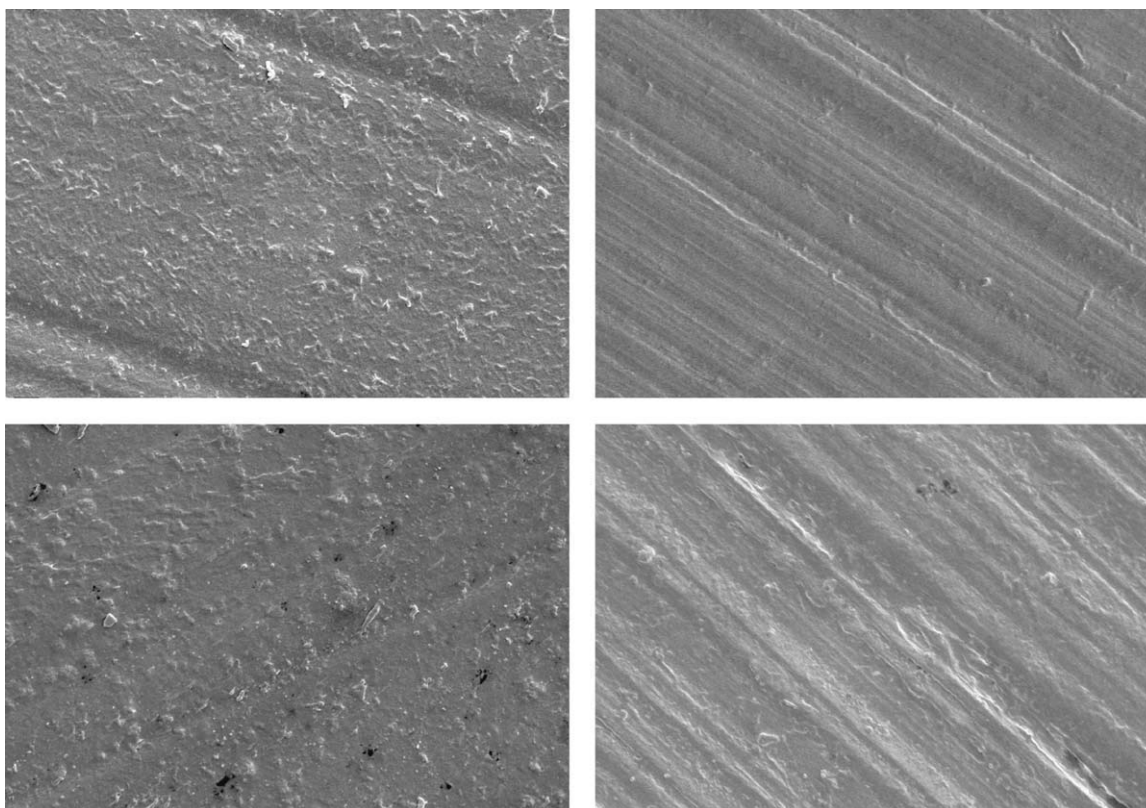


Figure 6 SEM micrographs of PC2 (top left), mPC2 (top right), PC15 (bottom left), and mPC15 (bottom right) tested using 7.5 N of normal force. Size of the displayed zones: $76.8 \times 56.4 \mu\text{m}^2$ (magnification: $\times 4000$).

reached. Figure 3 shows typical curves of friction force as a function of time. They correspond to PC8 and mPC8 and were obtained using 12.5 N of normal force. The behavior of the friction force of all material, with and without nanoparticles, is qualitatively similar.

The calculated friction coefficients are displayed in Figure 4 as a function of clay concentration. These data do not reveal significant dependency with clay concentration or normal load. According to these results, Amontons law is applicable to this polymeric system.¹² The average value of all friction coefficients displayed in Figure 4 is 0.35 ± 0.04 . Typically, the friction coefficients of polymeric systems are in the range 0.1–0.5.¹² Specifically, values of 0.28–0.4 have been reported for PP^{36–38} and of 0.2–0.6 for clay composites based in PET, PA-6, PBT, PP/PA blends, etc.^{17,39–42} The friction coefficients measured in this work are well in the range of those values. With respect to the effect of clay concentration in the value of the friction coefficient of the polymer, the results in the literature are not conclusive.²⁰ The addition of nanoparticles may produce the increase or the decrease of the friction coefficient, indicating that the friction mechanism is complex and that there may be competing factors associated with it. In the PP/PPg/o-MMT system considered in this work, the concentration of clay seems to have

no effect, at least in the range of concentrations covered.

Figures 5 and 6 display SEM micrographs of different final contact surfaces. They are representative of the type of surfaces found in the tested PNCs and their matrices. The micrographs in Figure 5, which correspond to PC5 and mPC5, were obtained using a $1000\times$ magnification, while those in Figure 6, that correspond to PC2, PC15 and their matrices, were obtained using a $4000\times$ magnification. The sliding of the pins against the metal disc produces tracks in the surfaces of all of the materials. In general, the PNC surfaces are rougher than those of the equivalent matrices. Moreover, a wavy morphology can be appreciated in all cases, but more noticeably in the composites. The photographs suggest that the wear mechanism is mainly abrasive, regardless of clay concentration and normal load used, although evidence of adhesive mechanism can also be appreciated, mainly in the surfaces of the matrices.

Figure 7 shows images of the surface of the counterbody obtained with an optical microscope. They correspond to disc 'B' after sliding samples of PP and PC5 with 7.5 and 12.5 N respectively. The photographs obtained with small magnifications (for example, $100\times$) show that the wear tracks left by PNCs are different than those of PP and the matrices. The former ones, which are represented by PC5

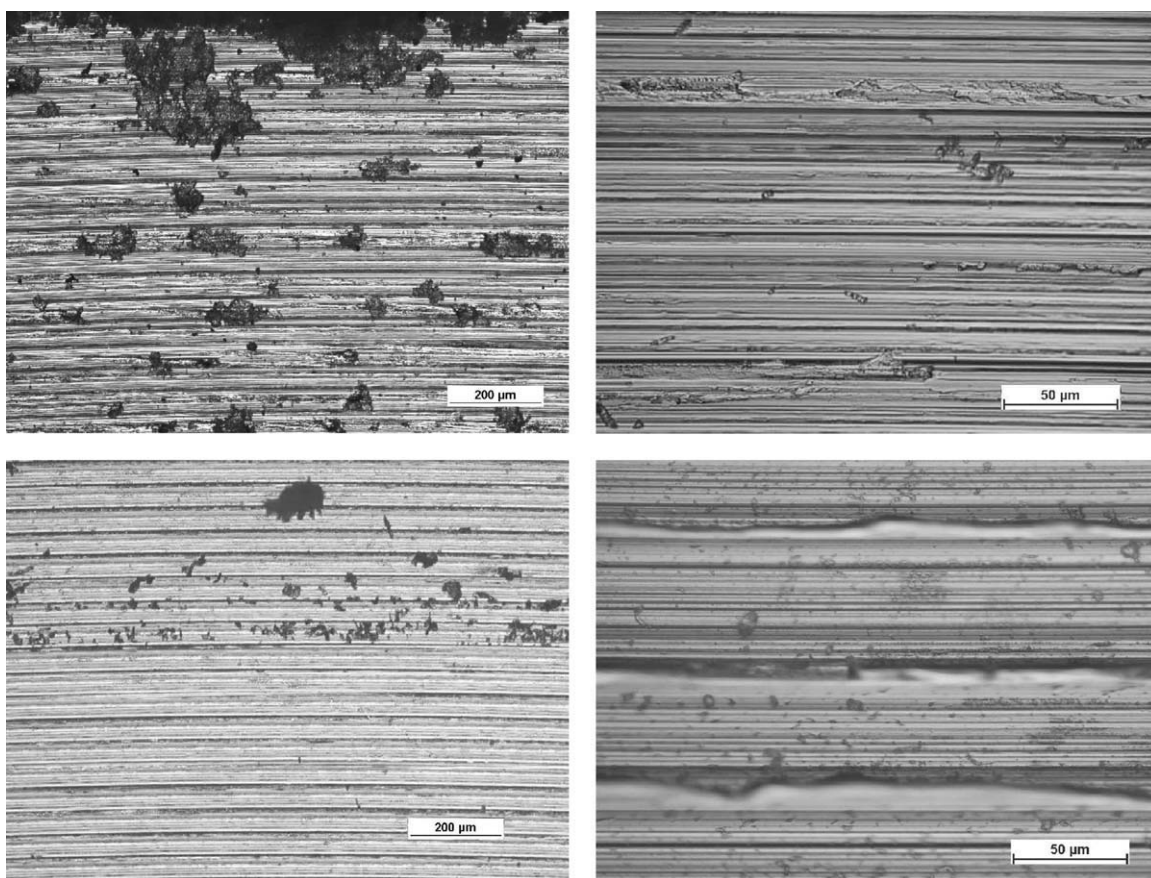


Figure 7 Optical micrographs of the counterbody after sliding tests of PP (top) and PC5 (bottom) at two magnifications: $\times 100$ (left) and $\times 500$ (right).

in Figure 7 (bottom left), display few fine debris particles in the pin track and small and dispersed polymeric particles outside the track border. In the case of PP and the matrices, large and thin plate-like debris particles remain in the pin track with large accumulations of those particles outside the pin trail (see, for example, the photograph of the track of PP in Figure 7 (upper left), where the border of the pin track is at the upper border of the photograph). However, larger magnifications reveal that everywhere along the track of all the different specimens, small fractions of polymeric material can be found that have been transferred to the metal counterface (photographs at the right of Fig. 7).

Permeability

Another property that may be improved by the presence of nanofillers is the gas permeability. Figure 8 displays the results of oxygen permeability of films of the PNCs and their matrices as a function of clay concentration. As expected, the permeability of PP is improved by the presence of silicate layers. This is caused by the retarded diffusion of the molecules which should follow more tortuous paths to bypass

the filler. Moreover, the data show that the oxygen permeability decreases as the clay concentration increases. The minimum value is obtained by PC15 which reaches practically 50% of the permeability of mPC15. Most authors that have studied PP/clay systems agree with this observation.^{5,28,29,43} It is

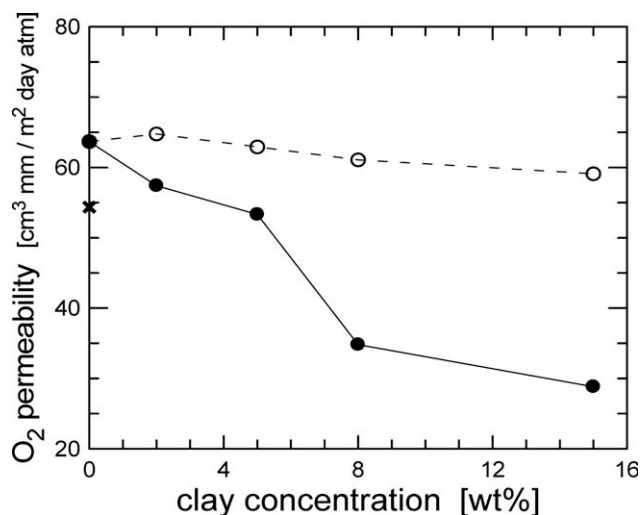


Figure 8 Oxygen permeability as a function of clay concentration. Symbols: (●), PNCs; (○), matrices; (×), PPg.

TABLE I
Melting Temperature (T_m) and Heat of Fusion (ΔH_m) of the Films Used in the Permeability Tests

Material	T_m (°C)	ΔH_m (J/g)
PP	166	89
PC2	165	89
mPC2	165	84
PC5	165	89
mPC5	165	90
PC8	164	91
mPC8	165	81
PC12	164	90
mPC12	164	85
PC15	164	88
mPC15	164	85

interesting to notice that the data suggest a change in behavior between PC5 and PC8. This observation reinforces the previous results from the rheological study of these materials⁸ that suggest that incipient percolation may occur in the range between 5 and 10 wt %. The data in Figure 8 also show that permeability of the PP/PPg matrices slightly decreases as the PPg concentration increases. This behavior may be expected since the permeability of the PPg, which is also included in the figure, is lower than that of PP.

The permeability of the nanocomposites is controlled by the structural characteristics of the matrix and the concentration and the degree of dispersion of the clay particles. The PNCs used in this work present a good dispersion of intercalated and exfoliated clay particles.^{8,9} Besides, all these materials display very similar fusion thermograms, which indicates comparable polymeric crystalline structure in all of them, regardless the concentration of clay (see temperature and heat of fusion data listed in Table I). Therefore, the decrease in permeability observed in the PNCs may be associated only to the amount of clay present.

CONCLUDING REMARKS

The effect of the organoclay concentration on the barrier and wear properties of PP/clay nanocomposites has been investigated. Clay concentrations from 2 to 15 wt % have been considered with a 3 : 1 PPg/o-MMT ratio. The results presented in this study validate the conclusion that the increase of the concentration of organoclay in the nanocomposites improves the wear resistant and the barrier properties of the materials.

The analysis of the contact surfaces suggest that the dominant wear mechanism observed in the performed pin-on-disk tests is mainly of the abrasive type, although evidence of adhesion was found while testing the PP and the matrices. Both the

PNCs and their matrices display wear resistance that decreases with normal load. For a given normal load, the wear rate of PP is augmented by the addition of PPg and reduced by the further incorporation of clay. As the clay concentration increases, the volume loss of the PNCs decreases. Contrary, the corresponding matrices display wear resistance that decrease as the PPg concentration increases. That is, the ratio of the wear rate of the PNCs with respect to their matrices becomes larger as the clay concentration increases reaching a maximum value of ~ 20 . Additionally, it was observed that the presence of clay as well as the magnitude of the applied load has no significant effect in the value of the friction coefficient of all analyzed materials. This coefficient was about 0.35.

The oxygen permeability of the PP gradually decreases with both, the addition of PPg and o-MMT. This barrier property reaches a maximum reduction of $\sim 55\%$ for PC15 and $\sim 10\%$ for its matrix, mPC15. This effect would be caused by the physical barrier imposed by the presence of the clay, since the morphology of all matrices is very similar according to the calorimetric measurements. Although all clay concentrations provide improved resistance by increasing the barriers for oxygen molecules to diffuse, the data suggest that a threshold is obtained at 5–8 wt %. This observation is in concordance with previous linear viscoelastic results⁸ that show evidence of percolation of clay tactoids at o-MMT concentrations between 5 and 10 wt %.

References

1. Utracki, L. A. Clay-Containing Polymeric Nanocomposites; Rapra Technology: Shawburi, 2004.
2. Okamoto, M. In *Macromolecular Engineering*; Matyjaszewski, K.; Gnanou, Y.; Leibler, L., Eds.; Wiley-VCH Verlag: Weinheim, 2007; p 2071.
3. Sinha Ray, S.; Okamoto, M. *Progr Polym Sci* 2003, 28, 1539.
4. Lotti, C.; Isaac, C. S.; Branciforti, M. C.; Alves, R. M. V.; Liberman, S.; Bretas, R. E. S. *Eur Polym J* 2008, 44, 1346.
5. Pannirselvam, M.; Genovese, A.; Jollands, M. C.; Bhattacharya, S. N.; Shanks, R. A. *eXPRESS Polym Lett* 2008, 2, 429.
6. Kanny, K.; Jawahar, P.; Moodley, V. K. *J Mater Sci* 2006, 43, 7230.
7. Kim, D. H.; Fasulo, P. D.; Rodgers, W. R.; Paul, D. R. *Polymer* 2007, 48, 5308.
8. Rohlmann, C. O.; Failla, M. D.; Quinzani, L. M. *Polymer* 2006, 47, 7795.
9. Rohlmann, C. O.; Horst, M. F.; Quinzani, L. M.; Failla, M. D. *Eur Polym J* 2008, 44, 2749.
10. Cassagnau, P. *Polymer* 2008, 49, 2183.
11. Lu, X.; Wang, K.; Chua, Y. C. In *Polyolefin Composites*; Nwabunma, D.; Kyu, T., Eds.; Wiley: New York, 2008; p 251.
12. Hutchings, I. M. *Tribology. Friction and Wear of Engineering Materials*; Arnold: London, 1996.
13. Bahadur, S. *Wear* 2000, 245, 92.
14. Rong, M. Z.; Zhang, M. Q.; Shi, G.; Ji, Q. L.; Wetzels, B.; Friedrich, K. *Tribol Int* 2003, 36, 697.
15. Bahadur, S.; Sunkara, C. *Wear* 2005, 258, 1411.

16. Bhimaraj, P.; Burris, D.; Sawyer, W. G.; Toney, C. G.; Siegel, R. W.; Schadler, L. S. *Wear* 2008, 264, 32.
17. Dasari, A.; Yu, Z. Z.; Mai, Y. W. *Mater Sci Eng* 2009, R63, 31.
18. Johnson, B. B.; Santare, M. H.; Novotny, J. E.; Advani, S. G. *Mech Mater* 2009, 41, 1108.
19. Finney Charles, D.; Gnanamoorthy, R.; Ravindrana, P. *Wear* 2010, 269, 565.
20. Zhang, Z.; Friedrich, K. In *Polymer Composites: From Nano to Macro-Scale*; Friedrich, K.; Fakirov, S.; Zhang, Z., Eds.; Springer: New York, 2005.
21. Chen, K.; Yang, R. C.; Cheng, S. W. *Tribology* 2006, 26, 561.
22. Kui, C.; Xiangdong, L.; Yuejun, S. *Lubrication Eng* 2008, 1, 110.
23. Kato, M.; Okamoto, H.; Hasegawa, N.; Tsukigase, A.; Usuki, A. *Polym Eng Sci* 2003, 43, 1312.
24. Krook, M.; Morgan, G.; Hedenqvist, M. S. *Polym Eng Sci* 2005, 45, 135.
25. Choudalakis, G.; Gotsis, A. D. *Eur Polym J* 2009, 45, 967.
26. Zhong, Y.; Janes, D.; Zheng, Y.; Hetzer, M.; de Kee, D. *Polym Eng Sci* 2007, 47, 1101.
27. Gorrasi, G.; Tortora, M.; Vittoria, V.; Kaempfer, D.; Mulhaupt, R. *Polymer* 2003, 44, 3679.
28. Villaluenga, J. P. G.; Khayet, M.; López-Manchado, M. A.; Valentin, J. L.; Seoane, B.; Mengual, J. I. *Eur Polym J* 2007, 43, 1132.
29. Mirzadeh, A.; Kokabi, M. *Eur Polym J* 2007, 43, 3757.
30. Sirousazar, M.; Yari, M.; Achachlouei, B. F.; Arsalani, J.; Mansoori, Y. *e-Polymers* 2007, 27, 1.
31. Mittal, V. J. *J Appl Polym Sci* 2008, 107, 1350.
32. Shafiee, M.; Ahmad Ramazani, S. A.; Danaei, M. *Plast Technol Eng* 2010, 49, 991.
33. Chinellato, A. C.; Vidotti, S. E.; Hu, G. H.; Pessan, L. A. *Compos Sci Technol* 2010, 70, 458.
34. Ramazani, S. A.; Tavakolzadeh, F.; Baniasadi, H. *J Appl Polym Sci* 2010, 115, 308.
35. Friedrich, K.; Lu, Z.; Hager, A. M. *Wear* 1995, 190, 139.
36. Steijn, R. P. In *Failure of Plastics*; Brostow, W.; Corneliussen, R. D., Eds.; Hanser: Munich, 1986; Chapter 19.
37. Ruiz, J. C.; Alvarez-Lorenzo, C.; Tabeada, P.; Burillo, G.; Bucio, E.; de Prijk, K.; Nelis, H. J.; Coenye, T.; Concheiro, A. *Eur J Pharmaceut Biopharm* 2008, 70, 467.
38. Mathew, M. T.; Novo, J.; Rocha, L. A.; Covas, J. A.; Gomes, J. R. *Tribol Int* 2010, 43, 1400.
39. Suresha, B.; Ravi Kumar, B. N.; Venkataramareddy, V.; Jayaraju, T. *Mater Design* 2010, 31, 1993.
40. Mu, B.; Wang, Q.; Wang, T.; Wang, H.; Jian, L.; Pei, X. *Polym Comp* 2009, 30, 619.
41. Kirupasankar, S.; Gnanamoorthy, R.; Velmurugan, R. *J Eng Trybol* 2010, 224, 133.
42. Mu, B.; Wang, Q.; Wang, T.; Wang, H.; Jian, L. *Polym Eng Sci* 2008, 48, 203.
43. Frounchi, M.; Dadbin, S.; Salehpour, Z.; Noferesti, M. *J Membr Sci* 2006, 282, 142.